UDC 621.396.962

ASSESSMENT OF THE QUALITY OF DETECTION OF A RADAR SIGNAL WITH NONLINEAR FREQUENCY MODULATION IN THE PRESENCE OF A NON-STATIONARY INTERFERING BACKGROUND

Hryzo A. A. – PhD, Associate Professor, Head of the Research Laboratory, Ivan Kozhedub Kharkiv National Air Force University, Kharkiv, Ukraine.

Kostyria O. O. – Dr. Sc., Senior Research, Leading Research Scientist, Ivan Kozhedub Kharkiv National Air Force University, Kharkiv, Ukraine.

Fedorov A. V. – PhD, Researcher, Ivan Kozhedub Kharkiv National Air Force University, Kharkiv, Ukraine.

Lukianchykov A. A. – Senior Researcher, Ivan Kozhedub National Air Force University, Kharkiv, Ukraine.

Biernik Ye. V. – Post-graduate student, Ivan Kozhedub Kharkiv National Air Force University, Kharkiv, Ukraine.

ABSTRACT

Context. Signals with long duration frequency modulation are widely used in radar, which allows increasing the radiated energy without degrading the range resolution and with peak power limitations. Increasing the product of the spectrum width by the radio pulse duration causes the passive interference zone to stretch out from the range, which leads to an interference with a more uniform intensity distribution in space and reduces the potential signal detection capabilities. Real passive obstacles have a non-stationary power distribution in space elements, so the signal reflected from the target can be detected in the gaps of passive obstacles or in areas with a lower level of them, provided that it is assessed (mapping of obstacles) and the detection threshold is adaptively set by space elements. Therefore, it is relevant to conduct research to assess the quality of detection of signals reflected from airborne targets depending on the level of non-stationarity of the interference background.

Objective. The aim of this work is to develop a methodology for assessing the influence of the level of the side lobes of signal correlation functions on the quality indicators of their detection in the presence of a non-stationary interference background of different intensity.

Method. The quality indicators of detection of frequency-modulated signals were studied. The problem of assessing the influence of the level of the lateral lobes of the correlation function on the quality indicators of signal detection against a non-stationary passive interference was solved by determining the parameters of the generalised gamma power distribution of such an interference, depending on the shape of the autocorrelation function of the signal.

Results. It is determined that for a high level of non-stationarity of the initial interference process for all signal models, the potential gain is almost the same and has a maximum value. In the case of reducing the level of non-stationarity of this process, the gain decreases. The traditional linear-frequency modulated signal gives a slightly worse result compared to nonlinear-frequency modulated signals. For all the studied frequency modulation laws, the gain is more noticeable when the requirements for signal detection quality are reduced.

Conclusions. A methodology for estimating the quality indicators of detecting echo signals on an interfering background with varying degrees of non-stationarity is developed. To improve the energy performance of detecting small-sized airborne objects against the background of non-stationary passive interference, it is advisable to use signals with nonlinear frequency modulation and reduce the probability of correct target detection.

KEYWORDS: detection of radar signals, nonlinear frequency modulation; side lobe level, non-stationary interference background.

ABBREVIATIONS

ACF is an autocorrelation function;
CF is a consistent filter;
FMR is a frequency modulation rate;
IPM is an intra-pulse modulation;
LFM is a linear frequency modulation;
LO is a local object;
ML is a main lobe;
MM is a mathematical model;
MSLL is a maximum side lobe level;
NLFM is a nonlinear frequency modulation;
NPI is a nonstationary passive interference;
PI is a passive interference;
Radar is a radar station (Radio Detection and Ranging);
SL is a side lobe;
SLL is a side lobe level.

NOMENCLATURE

$\dot{U}_{\Sigma}$ is a total complex amplitude of oscillations of a random process, V;

Δt is a sampling interval, s;

i, s is a range discrete number (space element);

$\dot{U}_N$ is a complex amplitude of oscillations of stationary noise, V;

σ_N^2 is a power of oscillations of stationary noise, dB;

$\dot{U}_{PI}$ is a complex amplitude of vibration of the PI, V;

$\sigma_{PI,i}^2$ is a power of oscillations of the PP in the i-*th* element of space, dB;

$\dot{U}_S$ is a complex amplitude of oscillations of the useful signal, V;

DOI 10.15588/1607-3274-2025-1-2

σ_S^2 is a power of oscillations of the useful signal, Db;

ξ is a weighting sum, V;

U is a voltage amplitude at the output of the CF, V;

D is a probability of correct target detection;

F is a likelihood of a false alarm;

ξ_0 is a target detection threshold level, V;

$W_{N,PI,S}(U)$ is a density of distribution of the additive mixture of noise, PI and signal;

$W_{N,PI}(U)$ is a distribution density of the additive mixture of noise and PI;

$W_{PI}(U/\lambda)$ is a conditional density of PI distribution;

λ is a vector of unknown parameters of the PI;

$W_{PI}(\dot{U})$ is an unconditional probability density of the PI;

$p(\lambda)$ is a density of the distribution of the vector of unknown parameters of the PI;

$D(q^2/\lambda)$ is a partial (fixed) indicator of target detection quality;

q^2 is a target detection parameter, dB;

$D(q^2)$ is an average quality of target detection;

$W(\sigma^2)$ is a generalized power distribution law of the PI;

α, c are parameters of the power distribution form the PI;

β is a power distribution scale parameter of the PI;

$G(z)$ is a gamma function;

$\langle\cdot\rangle$ is a statistical averaging operation;

m_1 is an average value of the PI power (first initial moment of distribution), V^2;

Δ is an average power fluctuation range of the PI relative to the average value, dB;

m_2 is a second initial moment of distribution, V^4;

k is a procedure of the law on power distribution of the PI;

q_i^2 is a parameter of target detection in the *i-th* element of space, dB;

ξ_i is a modular value of the weight sum in the *i-th* element of the space, V;

Δ_{Init} is an initial range of PI power fluctuations relative to the average value, dB.

INTRODUCTION

Attempts by manufacturers of modern radars to improve the characteristics of target detection and tracking in difficult signal and interference conditions while expanding the range of tasks they perform have led to the use of active digital antenna arrays [1–5]. The required values of mass, dimensions, reliability indicators of such systems and their functional flexibility can be achieved by using solid-state transmitting devices [1, 4, 5].

This technology has a significant disadvantage, namely, the limitation of the peak power of the sensing signals, which makes it difficult to achieve the required value of the maximum detection range. In order to overcome this drawback, the duration of signals is increased to ensure the required range of the radar, which in turn leads to an undesirable deterioration in range resolution. To overcome this contradiction, various types of IPM are used, usually linear, nonlinear frequency modulation and phase manipulation [6–8].

An analysis of the technical characteristics of radars available on the market and used by end users for airspace reconnaissance shows that they are all built on the above principle, with the actual differences being in the types of sensing signals used [7, 8].

A mandatory stage of processing complex sensing signals in the radar receiver is their compression into CF, which maximizes the signal-to-noise ratio and provides the required range resolution, which is determined by the width of the main peak of the filter response. The time-dependence of the CF response intensity is determined by its ACF, which, in addition to the ML, has SLs that can be quite long in time. In the case of detecting such compressed signals against the background of intrinsic noise, the influence of their SLs can be neglected. A different situation is observed when detecting such signals in ground surveillance radars, which almost always conduct airspace reconnaissance against the background of the SLs caused by the reflection of sounding signals from the earth's surface [9].

In the case of powerful PIs, the absolute level of the ACF SL will be significant. This leads to a stretching of the area of the PI, i.e., to the appearance of PIs in areas previously free of them, the overall level of non-stationarity of the interference background decreases. The targets previously observed in the interference gaps will be masked by the resulting background of the SL of compressed signals reflected from the PI from other areas of the range. In addition, when superimposing the SL of compressed signals reflected from long-range PIs that occupy several range discrete points, their level can reach significant values. This, in addition to an increase in the overall level of the interfering background, leads to the possibility of a multimode spectrum if reflections from different sources have different Doppler frequency shifts [6, 9].

Complex signals with NLFM have been widely used, and various authors have proposed a number of MMs of such signals with a reduced SL level of their ACF for practical application [10–33]. It seems expedient to evaluate the effect of the SL level of ACF on the quality indicators of signal detection against the background of non-stationary power PIs.

The object of study is the process of detecting NLFM signals in the background of the NPI.

The subject of study is the quality indicators for detecting NLFM signals on the background of NPI.

DOI 10.15588/1607-3274-2025-1-2

The purpose of the work is to development of a methodology for assessing the influence of the SLs of the ACF of complex signals on the quality indicators of their detection in the presence of a non-stationary background.

1 PROBLEM STATEMENT

We assume that a random process $\dot{U}_\Sigma$ is input to the receiver sequentially in time. Then the process is sampled in time with an interval Δt. From the absolute value of time $t = i \cdot \Delta t$, we proceed to indexing by the reference number i (the number of the range discrete).

We assume that the process in each i-th range discrete is the sum of independent normally distributed oscillations of the intrinsic stationary noise $\dot{U}_N$ with power $\sigma_N{}^2 = 1$, passive interference $\dot{U}_{PI}$ with known power $\sigma_{PI,i}{}^2$, and possibly a useful signal $\dot{U}_S$ with power $\sigma_S{}^2$:

$$\dot{U}_\Sigma = \dot{U}_N + \dot{U}_{PI} + \dot{U}_S .$$

We also assume that the random samples of the processes have a Rayleigh distribution of amplitude and a uniform distribution of the initial phase. Such a model corresponds to a signal reflected from a large number of randomly located, independently reflecting, equivalent shiny points and is appropriate for most practical situations.

The optimal detection algorithm is reduced to calculating the likelihood ratio or its logarithm [5, 7], which are monotonically increasing functions and describe the dependence of the likelihood ratio on the modular value of the normalized weighting sum ξ. Taking this into account, the optimal detection algorithm can be implemented by comparing the modular value of the weighting sum ξ with its threshold. Under the accepted conditions, the weighting operation can be performed by an optimal filter, and the value of the modular value of the weighting sum ξ is found as the amplitude of the voltage U at the filter output, which is subject to comparison with the threshold.

The conditional probability of correct detection D and false alarm F are most often used as indicators of detection quality. The detection characteristics D and F can be calculated as follows [5, 7]:

$$F = \int_{\xi_0}^{\infty} U \cdot \exp\left(-\frac{U^2}{2}\right) dU = \exp\left(-\frac{\xi_0{}^2}{2}\right), \qquad (1)$$

where the threshold level comes from

$$\xi_0 = \sqrt{2 \cdot \ln\left(\frac{1}{F}\right)} .$$

The conditional probability of correct detection is described by the expression:

$$D = \int_{\xi_0}^{\infty} W_{N,PI,S}(U)\,dU = \int_{\xi_0}^{\infty} l(U) \cdot W_{N,PI}(U)\,dU . \qquad (2)$$

Under real conditions, the distribution of the power of the PI by space elements is arbitrary and the value of their power $\sigma_{PI,i}{}^2$ is an unknown parameter with a certain distribution law.

Under such a priori uncertainty in the probability characteristics of signals and interference, the probability density of, for example, interference will be described by the conditional distribution density $W_{PI}(U/\lambda)$. Such a problem belongs to the class of problems with parametric a priori uncertainty [34]. The general approach to solving such problems [35] is to use the full probability formula to move from the conditional probability density $W_{PI}(\dot{U}/\lambda)$ to the unconditional probability density $W_{PI}(\dot{U})$:

$$W_{PI}(\dot{U}) = \int_{(\lambda)} W_{PI}(\dot{U}/\lambda) \cdot p(\lambda)\,d\lambda . \qquad (3)$$

The a priori uncertainty is associated with signal detection in different elements of space, where the parameters of the interference background may be different.

The combination of solutions (1), (2) in any discrimination elements with similar interference statistics allows obtaining, in fact, partial (fixed) quality indicators $D(q^2/\lambda)$, where q^2 determines the signal/interference+noise ratio. Moving to the average indicators $D(q^2)$ (similar to (3)), we obtain:

$$D(q^2) = \int_{(\lambda)} D(q^2/\lambda) \cdot p(\lambda)\,d\lambda , \qquad (4)$$

similarly, the detection threshold should be found from equation.

$$F = \int_{(\lambda)} F(\lambda) \cdot p(\lambda)\,d\lambda .$$

If we set the distribution density to $p(\lambda)$, the solution of a statistical problem under a priori uncertainty is reduced to solving it under known a priori conditions.

When choosing the type of distribution density of parameter λ, restrictions are imposed that are determined by the physical content and nature of the process, which narrows the range of acceptable distributions. Such restrictions may include, for example, the permissible range of parameter change, its mean value, variance, etc.

DOI 10.15588/1607-3274-2025-1-2

To move from the partial (conditional) to the average value of the probability of correct detection D, it is necessary to determine the distribution law that describes the statistical characteristics of the fixed parameter $\sigma_{PI,i}^2$. The generalized gamma distribution is used as the law of PI power distribution [35–39].

Further, we will take into account that in the case of a complex signal with IPM, the dependence of the CF response intensity will be determined by its ACF. The signal at each point in space will be an overlay of CF responses from neighboring range discrete samples, the number of components will be determined by the duration of the ACF signal, and their intensity – by the corresponding SL level. Obviously, the lower the SL level of the ACF, the less influence they have in the overall process, which in turn leads to a lower degree of reduction of the non-stationarity of the interference background and, accordingly, to better conditions for detecting signals reflected from targets against its background.

We will assume that the initial distribution of the PI intensity over the elements of space is determined by a gamma distribution with certain parameters, and in the case of superposition of SL reflections from different areas, taking into account the properties of the gamma function family, the total PI intensity distribution will also have a gamma distribution, but with different parameters.

Thus, the problem of assessing the effect of the SL of the ACF on the quality of signal detection against the background of the NPI can be solved by determining the parameters of the generalized gamma distribution of the PI power depending on the ACF signal shape and then averaging the partial detection rates in individual detection elements according to the law of PI intensity distribution, the parameters of which correspond to the selected IPM.

2 REVIEW OF THE LITERATURE

In [40], it is noted that radars that use compression methods for complex signals face the need to resolve conflicting requirements for pulse duration. Signals of short duration have good resolution, and long pulses are preferable in terms of ensuring maximum detection range. It is noted that when the pulse is compressed, unwanted SLs are present in the CF response, and their combined effect leads to inaccurate operation of detection systems. The authors of [41, 42] also point out that the use of complex signals avoids the problem of peak power limitation, but the presence of SLs in the CF output leads to the effect of masking weak signals, and it is noted that this effect can be quite significant and needs to be taken into account. To overcome this, algorithms for stabilizing the level of false alarms are proposed. A similar effect of SL masking weak targets by the total background of the PI of the compressed signal in the presence of powerful reflections from the PI is noted in [43]. To prevent this, methods of reducing the SLL of the compressed signal are proposed, which are based on the time analysis of the received signal and are implemented by selectively weighting the signal samples. In [44], it is proposed to use the median filtering procedure for this purpose. The common feature of the reviewed works is that the authors did not study the influence of the shape and SLL of the ACF signals on the detection quality indicators and do not provide their numerical values.

Papers [35–39] consider the family of generalized gamma distributions and show that the generalized gamma distribution is a continuous probability distribution with three parameters. It is a generalization of the two-parameter gamma distribution and is used for parametric approximation of data sets, including approximation of experimental signal power distributions.

The authors of [10–33] proposed a number of IPN laws that allow obtaining a low SLL of the ACF, so it is advisable to develop a method for assessing the degree of influence of the shape and SLL of the ACF on the quality indicators of signal detection against the background of the NPI.

3 MATERIALS AND METHODS

Let us consider the peculiarities of using the generalised power distribution law for the statistical description of the characteristics of the PI.

If it is desirable to use the experimental intensity distributions of passive interference $\sigma_{PI,i}^2$ in the input model, it is convenient to use the generalized power distribution law proposed for the first time in [36] (for simplicity, $\sigma_{PI,i}^2 = \sigma^2$ is assumed):

$$W\left(\sigma^2\right) = \frac{c \cdot \beta^{\alpha} \cdot \left(\sigma^2\right)^{\alpha-1}}{G\left(\frac{\alpha}{c}\right)} \cdot \exp\left(-\beta^c \cdot \left(\sigma^2\right)^c\right), \qquad (5)$$

provided that $\alpha > 0$, $c > 0$, $\beta > 0$.

This distribution generalizes a number of single-mode probabilistic models of radar reflectivity density distribution: log-normal, Weibull, K-distribution, exponential, Hoyt, Nakagami, Rayleigh, Rice, Beckman, uniform.

In practical applications, the power distribution of a power PI in space $\sigma_{PI,i}^2$ is often characterized by two parameters: the average power value $m_1 = \left\langle \sigma_{PI,i}^2 \right\rangle$ and the relative value Δ, which characterizes the average range of power fluctuations relative to the average value m_1:

$$\Delta = \frac{\sqrt{\left\langle \left(\sigma_{PI,i}^2 - \left\langle \sigma_{PI,i}^2 \right\rangle \right)^2 \right\rangle}}{m_1} = \frac{\sqrt{m_2 - m_1^2}}{m_1}. \qquad (6)$$

Usually, the value of m_1, referred to the intrinsic noise level, and the value Δ (6) are expressed in decibels.

DOI 10.15588/1607-3274-2025-1-2

For practical use, we will write the gamma density (5) in terms of the parameters m_1 and Δ. The formula for the initial moment of the k-th order of the distribution (5) is as follows [35, 36]:

$$m_k = G\left(\frac{\alpha+k}{c}\right)\Big/\left(\beta^k \cdot \Gamma\left(\frac{\alpha}{c}\right)\right). \quad (7)$$

In the case of k=1, this relation is converted into an expression for the mean power of a non-stationary random process $\left\langle \sigma_{PI,i}{}^2 \right\rangle = m_1$.

To approximate the experimental distributions of radar reflections power (selection of appropriate values of parameters α, c, β), the corresponding moments are equated, but in practice it is convenient to use the introduced values of m_1 and Δ, which is essentially equivalent to using the first two initial moments.

The probability distribution density (5) is a function of three parameters, and the number of moments to be compared is two, one parameter of the distribution law can be fixed: c=1.

In this case, the density (5) will be transformed into the density of the gamma distribution [35]:

$$W\left(\sigma^2\right) = \frac{\beta^\alpha \cdot \left(\sigma^2\right)^{\alpha-1}}{G(\alpha)} \cdot \exp\left(-\beta \cdot \sigma^2\right). \quad (8)$$

For the practical use of such a probabilistic model of fluctuations in the power of the PP, we define the parameters of the distribution density (8) α and β through the parameters m_1 and 3 (6).

Based on (7), taking into account that $G(\alpha+1) = \alpha \cdot G(\alpha)$, we obtain:

$$m_1 = \frac{G(\alpha+1)}{\beta \cdot G(\alpha)} = \frac{\alpha}{\beta},$$

$$\Delta = \frac{\sqrt{m_2 - m_1}}{m_1} = \sqrt{\frac{m_2}{m_1} - 1} = \sqrt{\frac{G(\alpha+2)\cdot G(\alpha)}{G(\alpha+1)^2} - 1} = \frac{1}{\sqrt{\alpha}}.$$

Invisible parameters α and β:

$$\alpha = \Delta^{-2},$$

$$\beta = \frac{\alpha}{m_1} = \frac{1}{m_1 \cdot \Delta^2}.$$

Finally, we write the density of the distribution (8) in the form (for simplicity, the index at m_1 is omitted since $m_1 \to m$):

$$W\left(\sigma^2, m, \Delta\right) = \frac{\left(\sigma^2\right)^{\Delta^{-2}-1}}{\left(m \cdot \Delta^2\right)^{\Delta^{-2}} \cdot G\left(\Delta^{-2}\right)} \cdot \exp\left(-\frac{\sigma^2}{m \cdot \Delta^2}\right). \quad (9)$$

The use of this law as a probabilistic model allows for a wide range of fluctuations in the power of PI Δ while maintaining its average value m.

Let's estimate the effect of the level of obstacle non-stationarity on the quality of useful signal detection.

To simplify the calculations (by fixing the false alarm level F) under the influence of a non-stationary interference background, it is advisable to use the modular value of the weighting sum ξ_i as a sufficient statistic. It is known that in this case, the response in the absence of a useful signal and Gaussian interference has a Rayleigh distribution with unit variance $\sigma_{PI,i}{}^2$.

Assuming that each i-th element of the space has its own modular value of the weighting sum ξ_i, for a signal with a random amplitude distributed according to Rayleigh's law and a uniformly distributed initial phase, we have [5, 7]:

$$D_i = F^{\frac{1}{1+\frac{q_i^2}{2}}}, \quad (10)$$

and $q_i{}^2$ defines the signal/interference+noise ratio in the i-th element of space. For the specified conditions, the detection parameter is equal to [5, 7]:

$$q_i{}^2 = 2 \cdot \frac{\sigma_S{}^2}{\sigma_N{}^2 + \cdot \sigma_{PI,i}{}^2}. \quad (11)$$

In another similar (s-th) element of space, the detection parameter $q_s{}^2$ will differ only by a different, but known for this element, intensity value $\sigma_{PI,s}{}^2$.

To move from the partial (conditional) to the average value of the probability of correct detection D, it is necessary to set the distribution laws that describe the statistical characteristics of parameter $\sigma_{PI,i}{}^2$.

As a probabilistic model of PI power fluctuations, we use the generalized gamma power distribution (5), (8), (9). Then, the average value of the probability of correct detection, taking into account (5), (9), (10) and (11), is written as follows:

$$D = \int_0^\infty F^{\left(1+\frac{\sigma_c{}^2}{\sigma_N{}^2+\sigma_{PI,i}{}^2}\right)^{-1}} \cdot W\left(\sigma_{PI,i}{}^2, m, \Delta\right) d\sigma_{PI,i}{}^2. \quad (12)$$

Expression (12) makes it possible to estimate the efficiency of detecting a useful echo signal under different variants of input influences. By varying the value of Δ at a fixed level of the average power of the PI m, it is possible to obtain detection quality indicators corresponding to different degrees of non-stationarity of the interfering

DOI 10.15588/1607-3274-2025-1-2

background. For $\Delta \to -\infty$, we obtain the detection quality indicators corresponding to a stationary interference background.

4 EXPERIMENTS

Let us evaluate the effect of the SL of the ACF on the quality of echo detection against the background of the NPI in terms of reducing the relative level of fluctuations Δ (6) of their intensity distribution in space.

In Figure 1, the solid line shows the energy relief of the PI by range, and the dashed line shows the result of modelling the response of the signal compression filter with an LFM, the first SLs of the ACF which are –13 dB relative to the level of the ML, and the duration is 120 range samples. To preserve the energy relations, the processes are normalized in such a way as to ensure the equality of the average value of the PI intensity.

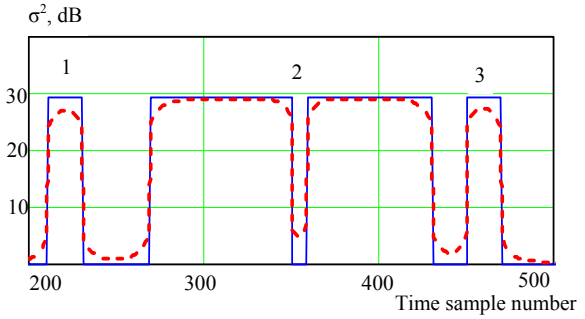

Figure 1 – Passive interference intensity distribution by range sweep

The abscissa axis is the number of range samples, and the ordinate axis is the signal intensity, referred to the intrinsic noise level in decibels. For simplicity, it is assumed that the intensity of the reflections from the LO is the same and is 30 dB (solid line in Figure 1). Figure 1 shows the situational marks 1, 2, 3, which will be discussed further.

Situation 1 corresponds to the presence of a separately located point reflection from the LO, when the distance to the next area occupied by the PI exceeds the duration of the probing signal. Situations 2, 3 correspond to the presence of closely spaced areas of the PI when the distance between them is less than the duration of the probing signal.

When observing a weak target echo, the absolute value of the compressed signal SLL will be lower than the level of the receiver's own noise, but in the case of powerful reflections from the PI, this level will be significant. For example, for the selected case, when the PI with a power of 30 dB is affected, the absolute value of the SLL will be 15...17 dB relative to the level of the receiving path's own noise. This leads to the stretching of the area of the PI action, i.e., to the appearance of PIs in areas previously free of them, in addition, when the SL superimposes compressed signals reflected from long-range PIs occupying several range discrete values, their level can reach significant values (situation 1, 2, 3 areas to the left and right of the PI location). Situation 2 differs from Situation 1 in that the SLs of compressed signals from different areas occupied by the PI overlap, which leads to an increase in the overall level of interference background in previously free areas and the possibility of a multimode spectrum if reflections from different sources have different Doppler frequency shifts. Situation 3 corresponds to the case of the end of the range of the PI, we see that the area occupied by the PI is extended to the duration of the sensing signal, the additional increase is 120 range discrete.

Figure 1 is for illustrative purposes only and confirms that the signal at each point in space will be an overlay of CF responses from neighboring range discrete samples, the number of components will be determined by the duration of the ACF signal, and their intensity will be determined by the corresponding SL level. Obviously, the lower the level of the SL of the ACF, the less influence they have in the overall process, which in turn leads to a lower degree of reduction of the interference background non-stationarity and, accordingly, better conditions for detecting echo signals against it.

Next, let's consider the quality indicators of echo detection for three models of signals with IPM.

We will consider the MM of the NLFM signals introduced in [10–13], consisting of two and three LFM fragments, which compensate for jumps in instantaneous frequency and phase that occur at the moments of change in the FMR when moving from one signal fragment to another. The use of these models ensures the disappearance of the distortion of the shape of their spectra, which leads to a decrease in the MSLL of their ACF. To compare the results, we will use a classical LFM signal of the same duration.

We will evaluate the impact of the SLL of the ACF of the selected signal models by simulation. We will use a test implementation of the NPI intensity distribution by range elements with known parameters m and Δ. The output sequence will be determined by summing the CF responses from the corresponding range discrete elements. The CF response will be determined by the intensity of the signal and its ACF value at certain moments of time; for ease of use, the ACF characteristics of the signals to be compared are given in Table 1.

Table 1 shows the values of the MSLL and the decay rate of the SLL of their ACFs of two- and three-fragment NLFM signals (models 1 and 2, respectively) and the classical LFM signal (model 3). The values of the relative level of fluctuations Δ at the output of the CF of the corresponding type of signal for three variants of the value of the relative level of fluctuations of the initial process Δ_{Init} are presented. The average power of the processes is the same m=10 dB. Thus, it is possible to estimate the reduction of the degree of non-stationarity of the initial process and the potential losses from this. The signals of all models have the same duration.

The ACF signals from Table 1 are shown in Figures 2, 3, 4.

DOI 10.15588/1607-3274-2025-1-2

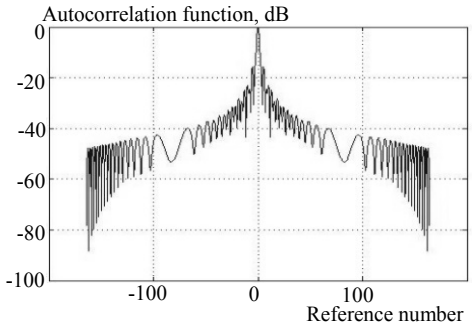

Figure 2 – ACF of a two-fragment NLCM signal (model No.1)

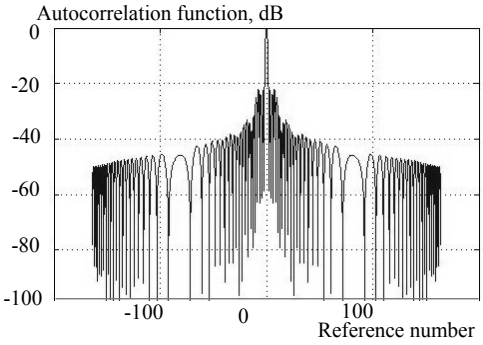

Figure 3 – ACF of a three-fragment NLCM signal (model No.2)

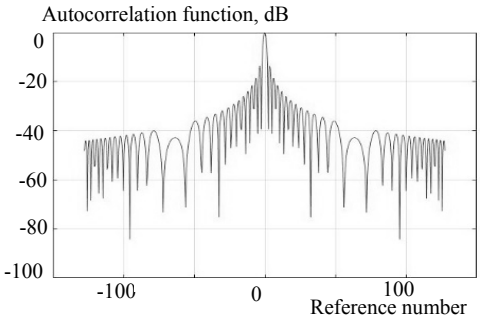

Figure 4 – ACF of the LFM signal (model №3)

Table 1 – Characteristics of the ACF signal models and simulation results

No	MM of the signal	MSLL, dB	Decrease in MRBP, dB/dec	Δ, dB		
				Δ_{Init} = =10.23	Δ_{Init} = =5.03	Δ_{Init} = =3.05
1.	LFM–LFM	–15.81	20.00	8.89	3.45	1.03
2.	LFM–LFM–LFM	–22.00	19.30	9.78	4.52	2.43
3.	LFM	–13.00	22.00	8.78	3.33	0.92

5 RESULTS

The results of the evaluation of the quality indicators of detecting fingerprints against the background of PI with different levels of non-stationarity according to (9), (12) for the signals of the selected models (Table 1) are shown in Figures 5 a,b,c as a function of the conditional probability of correct detection on the signal intensity.

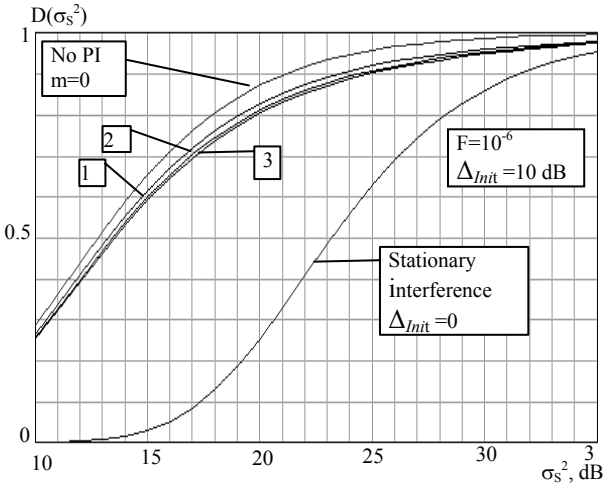

a) background instability level Δ_{Init} = 10 dB

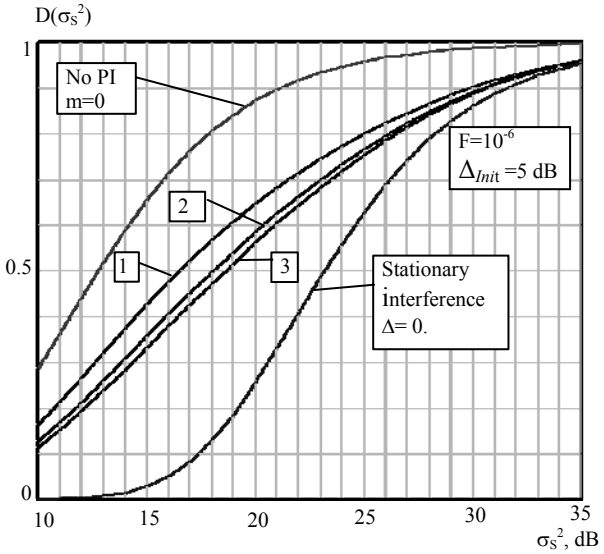

b) background instability level Δ_{Init} = 5 dB

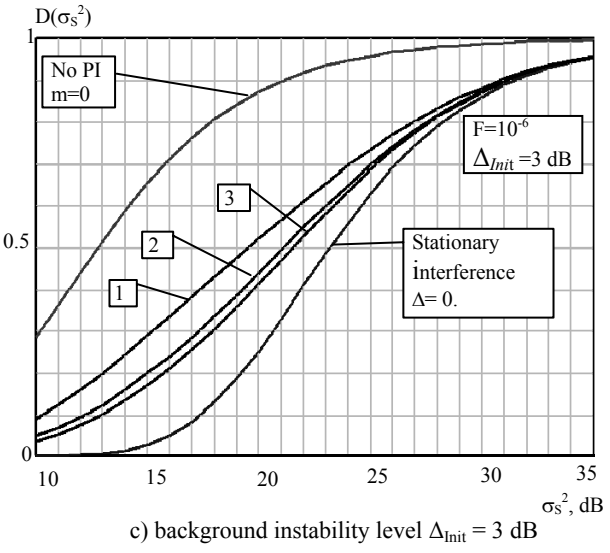

c) background instability level Δ_{Init} = 3 dB

Figure 5 – Detection curves for different signal models

DOI 10.15588/1607-3274-2025-1-2

The corresponding model numbers are shown in the figures and correspond to the numbering in Table 1. The curves are plotted for the case of average interference power m=10 dB and conditional false alarm probability F=10^{-6}. For comparison, two extreme cases are presented – no interference and the presence of a stationary interference with an intensity of 10 dB. Model No. 3 corresponds to the use of a traditional LFM signal.

6 DISCUSSION

The analysis of the figures shows that a higher level of non-stationarity of the initial process corresponds to a greater gain in the signal/interference+noise ratio that can potentially be obtained. In Figure 5a, the level of non-stationarity of the initial process is Δ_{Init} = 10 dB, for all signal models (curves 1, 2, 3), the potential gain is almost the same and amounts to 9 dB. This can be explained by the fact that with such a significant level of non-stationarity, virtually all the interference power is concentrated in a few range areas, while other areas are free from its influence. Under these conditions, the shape of the ACF and its MSLL does not play a major role, in fact, it is a matter of detecting point targets against the background of their own noise. The difference in the curves is no more than 0.3 dB.

With a decrease in the level of non-stationarity of the initial process, the influence of the ACF shape and its MSLL becomes more significant. This can be explained by the fact that the areas occupied by the PIs begin to occur more frequently, and the effect of the overlapping of the SL responses from different range areas becomes more significant. For the curves corresponding to models 1 and 2, the gain is 5–6 dB for the case of Δ_{Init} = 5 dB and 2–3 dB for ΔInit = 3 dB. The decrease in gain for a lower level of background non-stationarity is explained by its approach to the stationary one.

It should be noted that the traditional LFM yields a worse result by 0.5–0.7 dB compared to two- and three-fragment NLFM signals in terms of providing a potential energy gain when detecting targets against a non-stationary interference background. This is as it should be, given the higher integral SL level of its ACF.

For all cases, the gain is more noticeable with low requirements for signal detection quality (D<0.5) and can be 6–7 dB.

CONCLUSIONS

The paper investigates the quality indicators of detection of FM radar signals against the background of NPI formed by time-superimposed CF responses caused by the SLs of the ACF of these signals.

The scientific novelty lies in the development of a methodology for assessing the quality of detection of echo signals against an interfering background with varying degrees of non-stationarity, the essence of which, unlike the known ones, is to determine the parameters of the generalized gamma distribution of the power of the NPI depending on the shape of the ACF signal. For this purpose, we use the averaging of partial detection rates in individual detection elements according to the law of the intensity distribution of the PP and taking into account the parameters of the law of the FM signals. This technique is applied to the study of two- and three-fragment NLFM signals and a signal with LFM.

The practical significance of The conclusion of the obtained results is the possibility of using the proposed methodology for assessing the quality indicators of detecting echo signals on an interference background with varying degrees of non-stationarity for comparative analysis of NLFM signals with different FM laws. The results obtained allow us to conclude that in order to improve the energy performance of detecting small-sized targets, it is advisable to reduce the probability of correct target detection below the value of 0.5.

Prospects for further research it is planned to study the previously developed MMs of two- and three-fragment NLFM signals for the expediency of their application in various radar models to optimise their operating modes.

ACKNOWLEDGEMENTS

We thank the management of Ivan Kozhedub Kharkiv National Air Force University for the opportunity to conduct scientific research.

REFERENCES

1. Richards M. A., Scheer J., Holm W. A. Principles of modern radar. Basic principles. Sci Tech Pub, 2010, 924 p.
2. Blackman S. S., Popoli R. F. Design and analysis of modern tracking systems. Boston, London, Artech House, 1999, 1230 p.
3. You H., Jianjuan X., Xin G. Radar data processing with applications. House of electronics industry publishers, 2016, 536 p. DOI:10.1002/9781118956878
4. Melvin W. L., Scheer J. A. Principles of Modern Radar. Vol. II: Advanced Techniques. Sci Tech Publishing, 2013, 846 p.
5. Barton D. K. Radar system analysis and modeling. Boston, London, Artech House Publishers, 2004, 566 p.
6. Van Trees H. L. Detection, estimation, and modulation theory. Part III: Radar-Sonar processing and Gaussian signals in noise. John Wiley & Sons, Inc., 2001, 643 p. DOI: 10.1002/0471221090
7. Levanon N., Mozeson E . Radar signals. New York, John Wiley & Sons, Inc., 2004, 403 p.
8. Cook C. E., Bernfeld M. Radar signals: An introduction to theory and application. Boston, Artech House, 1993, 552 p.
9. McDonough R. N., Whalen A. D. Detection of signals in noise (2nd. Ed.). San Diego, Academic Press, Inc., 1995, 495 p.
10. Kostyria O. O. , Hryzo A. A. , Dodukh O. M. et al. Mathematical model of a two-fragment signal with a non-linear frequency modulation in the current period of time, V*isnyk NTUU KPI Seriia – Radiotekhnika Radioaparatobuduvannia,* 2023, Vol. 92, pp. 60–67. DOI:10.20535/RADAP.2023.92.60-67.
11. Kostyria O. O., Hryzo A. A., Dodukh O. M. et al. Improvement of mathematical models with time-shift of two- and tri-fragment signals with non-linear frequency modulation, *Visnyk NTUU KPI Seriia – Radiotekhnika Radioaparatobudu-*

DOI 10.15588/1607-3274-2025-1-2

vannia, 2023, Vol. 93, pp. 22–30. DOI: 10.20535/RADAP.2023.93.22-30.
12. Kostyria O. O. , Hryzo A. A. , Khizhnyak I. A. et al. Implementation of the method of minimizing the side lobe level of autocorrelation functions of signals with nonlinear frequency modulation, *Visnyk NTUU KPI Seriia – Radiotekhnika Radioaparatobuduvannia*, 2024, Vol. 95, pp. 16–22. DOI: 10.20535/RADAP. 2024.95.16-22
13. Kostyria O. O. , Hryzo A. A. , Solomonenko Yu. S. et al. Mathematical model of shifted time of combined signal as part of fragments with linear and quadratic frequency modulation, *Visnyk NTUU KPI Seriia – Radiotekhnika Radioaparatobuduvannia*, 2024, Vol. 97, pp. 5–11. DOI:10.20535/RADAP.2024.97.5-11
14. Adithya V. N., Elizabath R. D., Kavitha C. Modified radar signal model using NLFM, *International Journal of Recent Technology and Engineering (IJRTE)*, 2019, Vol. 8, Issue 2S3, pp. 513–516. DOI: 10.35940/ ijrte.b1091.0782s319
15. Anoosha Ch., Krishna B. T. Peak sidelobe reduction analysis of NLFM and improved NLFM radar signal with non-uniform PRI, *Aiub Journal of Science and Engineering (AJSE)*, 2022, Vol. 21, Issue 2, pp. 125–131.
16. Zhaoa Yu. , Ritchieb M. , Lua X. et al. Non-continuous piecewise nonlinear frequency modulation pulse with variable sub-pulse duration in a MIMO SAR radar system, *Remote Sensing Letters,* 2020, Vol. 11, Issue 3, pp. 283–292. DOI: 10.1080/2150704X.2019 .1711237
17. Van-Zyl A. C. , Wiehahn E. A. , Cillers J. E. et al.]Optimized multi-parameter NLFM pulse compression waveform for low time-bandwidth radar, *International Conference on Radar Systems*, 2022, pp. 289–294. DOI: 10.1049/icp.2022.2332.
18. Fan Z., Meng H. Coded excitation with nonlinear frequency modulation carrier in ultrasound imaging system, *2020 IEEE Far East NDT New Technology & Application Forum.* Kunming, Yunnan province, China, conference paper, IEEE, 2020, pp. 31–35. DOI: 10.1109/FENDT50467.2020.9337517.
19. Adithya V. N., Elizabath R. D., Kavitha C. Performance analysis of NLFM signals with Doppler effect and background noise, *International Journal of Engineering and Advanced Technology (IJEAT)*, 2020, Vol. 9, Issue 3, pp. 737–742. DOI: 10.35940/ijeat. B3835.029320
20. Zhang Y., Deng Y., Zhang Z. et al. Analytic NLFM waveform design with harmonic decomposition for synthetic aperture radar, *IEEE Geoscience and Remote Sensing Letters,* 2022, Vol. 4, Article no 4513405. DOI: 10.1109/lgrs.2022.3204351
21. Xie Q., Zeng H., Mo Z. et al. A two-step optimization framework for low sidelobe NLFM waveform using fourier series, *IEEE Geoscience and Remote Sensing Letters,* 2022, Vol. 19, Article no 4020905. DOI: 10.1109/LGRS.2022.3141081
22. [Zhuang R., Fan H., Sun Y. et al. Pulse-agile waveform design for nonlinear FM pulses based on spectrum modulation, IET International Radar Conference, 2021, pp. 964–969. DOI: 10.1049/icp.2021.0700.
23. Shuyi L. , Jia Y. , Liu Y. et al. Research on ultra-wideband NLFM waveform synthesis and grating lobe suppression, *Sensors*, 2022, No. 24, Article number 9829. DOI: 10.3390/s22249829
24. Swiercz E., Janczak D., Konopko K. Estimation and classification of NLFM signals based on the time-chirp, *Sensors*, 2022, Vol. 22, Issue 21, Article no 8104. DOI: 10.3390/s22218104
25. Saleh M. , Omar S.-M. , Grivel E. et al. A variable chirp rate stepped frequency linear frequency modulation waveform designed to approximate wideband non-linear radar waveforms, *Digital Signal Processing,* 2021, Vol. 109, Article no 102884, 19 p. DOI: 10.1016/j.dsp.2020.102884
26. Xu Z., Wang X. , Wang Y. Nonlinear frequency-modulated waveforms modeling and optimization for radar applications, *Mathematics*, 2022, Vol. 10, P. 3939. DOI: 10.3390/math10213939.
27. Widyantara M. R. , Suratman S.-F. Y. , Widodo S. et al. Analysis of non linear frequency modulation (NLFM) waveforms for pulse compression radar, *Jurnal Elektronika dan Telekomunikasi*, Vol. 18, Issue 1, pp. 27–34. DOI: 10.14203/jet.v18.27-34
28. Ping T., Song C., Qi Z. et al. PHS: A pulse sequence method based on hyperbolic frequency modulation for speed measurement, *International Journal of Distributed Sensor Networks*, 2024, Vol. 2024, Article no 6670576, 11 p. DOI:10.1155/2024/6670576
29. Cheng Z., Sun Z. , Wang J. et al. Magneto-Acousto-Electrical Tomography using Nonlinearly Frequency-Modulated Ultrasound, *Phys. Med. Biol.,* 2024, Vol. 69(8), PMID: 38422542. DOI:10.1088/1361-6560/ad2ee5
30. Singh A. K., Bae K.-B., Park S.-O. NLFM pulse radar for drone detection using predistortion technique, *Journal of Electromagnetic Waves and Applications*, 2021, Vol. 35, pp. 416–429.
31. Septanto H., Sudjana O., Suprijanto D. A novel rule for designing tri-stages piecewise linear NLFM chirp, *2022 International Conference on Radar, Antenna, Microwave, Electronics, and Telecommunications (ICRAMET), Bandung, 6–7 December 2022*. Indonesia, IEEE, 2022, pp. 62–67. DOI: 10.1109/ICRAMET 56917.2022.9991201
32. Kostyria O. O., Hryzo A. A. , Dodukh O. M. Combined two-fragment radar signals with linear and exponential frequency modulation laws, *Systems of Arms and Military Equipment*, 2024, № 4 (76), pp. 58–64. DOI: 10.30748/soivt.2023.76.06
33. Kostyria O. O., Hryzo A. A. , Dodukh O. M. Synthesis time-shifted mathematical model of a combined signal with linear and cubic frequency modulation, *Information Processing Systems*, 2024, № 1 (176), pp. 73–81. DOI:10.30748/soi.2024.176.09
34. Kaliuzhnyi M. , Semenets V. , Orlenko V. et al. Synthesis of a single-channel device for receiving and primary signal processing under conditions of structural-parametric a priori uncertainty, *2022 IEEE 2nd Ukrainian Microwave Week (UkrMW)*. Ukraine, IEEE, 2022, pp. 573–578. DOI: 10.1109/UkrMW58013.2022. 10037164
35. Feller W. An introduction to probability theory and its applications, Volume 2 / W. Feller. – New York: John Wiley & Sons Inc., 1991. – 683 p.
36. Stacy E. W. A generalization of the gamma distribution, Annals of Mathematical Statistics, 1962, Vol. 33(3), pp. 1187–1192. DOI: 10.1214/aoms/ 1177704481
37. Alzaatreh A., Lee C. & Famoye F. Family of generalized gamma distributions: Properties and applications, *Hacettepe Journal of Mathematics and Statistics,* 2016, Vol. 45(3), pp. 869–886. DOI:10.15672/ HJMS.20156610980
38. Kiche J., Ngesa O. & Orwa G. On generalized gamma distribution and its application to survival data, *International Journal of Statistics and Probability,* 2019, Vol. 8(5), pp. 85–102. DOI: 10.5539/ijsp.v8n5p85
39. Sportouche H., Nicolas J.-M., Tupin F. Mimic capacity of fisher and generalized gamma distributions for high-

DOI 10.15588/1607-3274-2025-1-2

resolution SAR image statistical modeling, *IEEE Journal of Selected Topics in Applied Earth Observations and Remote Sensing*, 2017, Vol. 10, Issue 12, pp. 5695–5711.
40. Thakur A. and Saini D. S Transmit waveform design to avoid target masking in pulse compression radar, *2020 International Conference on Communication and Signal Processing (ICCSP)*, Chennai. India, 2020, pp. 97–101. DOI:10.1109/ICCSP48568.2020. 9182221
41. Zhu X. , He F. , Ye F. et al. Sidelobe suppression with resolution maintenance for SAR images via sparse representation, *Sensors (Basel),* 2018, Vol. 18(5), Article no1589. DOI: 10.3390/s18051589; PMID: 29772743; PMCID: PMC5982680.
42. Haliloglu O., Yilmaz A. O. Successive target cancelation in pulse compression radars, *2007 IEEE Radar Conference, Waltham*. MA, USA, IEEE, 2007, pp. 885–890. DOI: 10.1109/RADAR.2007.374336
43. Nepal R. , Li Z. , Zhang Y. et al. A simulation of study of the impact of surface clutter on spaceborne precipitation radar sensor, *In Proceedings of the 36th Conference on Radar Meteorology*. Breckenridge, CO, USA: IEEE, 2013, pp. 16–20.
44. Maki M., Kobori T. Construction of three-dimensional weather radar data from volcanic eruption clouds, *MethodsX,* 2021, Vol. 8, Article no 101535. DOI: 10.1016/j.jvolgeores.2021.107178

Received 12.11.2024.
Accepted 26.01.2025.

УДК 621.396.962

ОЦІНКА ЯКОСТІ ВИЯВЛЕННЯ РАДІОЛОКАЦІЙНОГО СИГНАЛУ З НЕЛІНІЙНОЮ ЧАСТОТНОЮ МОДУЛЯЦІЄЮ ЗА НАЯВНОСТІ НЕСТАЦІОНАРНОГО ПЕРЕШКОДОВОГО ФОНУ

Гризо А. А. – канд. техн. наук, доцент, начальник НДЛ Харківського національного університету Повітряних Сил імені Івана Кожедуба, Харків, Україна.

Костиря О. О. – д-р техн. наук, старший науковий співробітник, провідний науковий співробітник Харківського національного університету Повітряних Сил імені Івана Кожедуба, Харків, Україна.

Федоров А. В. – д-р філос., науковий співробітник Харківського національного університету Повітряних Сил імені Івана Кожедуба, Харків, Україна.

Лук'янчиков А. А. – старший науковий співробітник Харківського національного університету Повітряних Сил імені Івана Кожедуба, Харків, Україна.

Бєрнік Є. В. – ад'юнкт Харківського національного університету Повітряних Сил імені Івана Кожедуба, Харків, Україна.

АНОТАЦІЯ

Актуальність. В радіолокації широке застосування знайшли сигнали з частотною модуляцією великої тривалості, що дозволяє без погіршення роздільної здатності за дальністю збільшити випромінювану енергію при обмеженнях на пікову потужність. Збільшення добутку ширини спектру на тривалість радіоімпульсу викликає розтягування зони пасивних перешкод з дальності, що призводить до появи перешкоди з більш рівномірним розподілом інтенсивності у просторі та знижує потенційні можливості з виявлення сигналу. Реальні пасивні перешкоди мають нестаціонарний розподіл потужності в елементах простору, за таких умов відбитий від цілі сигнал можна виявляти у розривах пасивних перешкод або на ділянках з меншим їх рівнем за умови його оцінювання (ведення карти перешкод) та адаптивного встановлення порогу виявлення за елементами простору. Тому є актуальним проведення досліджень з оцінки якості виявлення відбитих від повітряних цілей сигналів у залежності від рівня нестаціонарності перешкодового фону.

Метою роботи є розробка методики для оцінки впливу рівня бічних пелюсток функцій кореляції сигналів на показники якості їх виявлення при наявності нестаціонарного перешкодового фону різної інтенсивності.

Метод. Досліджувалися показники якості виявлення частотно-модульованих сигналів. Задачу оцінки впливу рівня бічних пелюсток функції кореляції на показники якості виявлення сигналів на фоні нестаціонарної пасивної перешкоди вирішено шляхом визначення параметрів узагальненого гама-розподілу потужності такої перешкоди в залежності від форми автокореляційної функції сигналу.

Результати. Визначено, що для високого рівня нестаціонарності початкового перешкодового процесу для усіх моделей сигналів потенційний виграш майже однаковий та має максимальне значення. У разі зниження рівня нестаціонарності цього процесу виграш зменшується. Традиційний лінійно-частотно модульований сигнал дає у порівнянні з нелінійно-частотно модульованими сигналами дещо гірший результат. Для всіх досліджених законів частотної модуляції виграш більш відчутний за зниження вимог до показників якості виявлення сигналу.

Висновки. Розроблено методику оцінки показників якості виявлення луна-сигналів на перешкодовому фоні з різним ступенем нестаціонарності. Для покращення енергетичних показників виявлення малорозмірних повітряних об'єктів на фоні нестаціонарних пасивних перешкод доцільно застосовувати сигнали з нелінійною частотною модуляцією та знижувати значення ймовірності правильного виявлення цілей.

КЛЮЧОВІ СЛОВА: виявлення радіолокаційних сигналів, нелінійна частотна модуляція; рівень бічних пелюсток, нестаціонарний перешкодовий фон.

DOI 10.15588/1607-3274-2025-1-2

ЛІТЕРАТУРА

1. Richards M. A. Principles of modern radar. Basic principles / M. A Richards, J. Scheer, W. A. Holm. – Sci Tech Pub, 2010. – 924 p.
2. Blackman S. S. Design and analysis of modern tracking systems / S. S. Blackman, R. F. Popoli. – Boston; London: Artech House, 1999. – 1230 p.
3. You H. Radar data processing with applications / H. You, X. Jianjuan, G. Xin. – House of electronics industry publishers, 2016. – 536 p. DOI:10.1002/9781118956878
4. Melvin W. L. Principles of Modern Radar. Vol. II: Advanced Techniques / W. L. Melvin, J. A. Scheer. – Sci Tech Publishing, 2013. – 846 p.
5. Barton D. K. Radar system analysis and modeling / D. K. Barton. – Boston; London: Artech House Publishers, 2004. – 566 p.
6. Van Trees H. L. Detection, estimation, and modulation theory. Part III: Radar-Sonar processing and Gaussian signals in noise / H. L. Van Trees. – John Wiley & Sons, Inc., 2001. – 643 p. DOI: 10.1002/0471221090
7. Levanon N. Radar signals / N. Levanon, E Mozeson. – New York: John Wiley & Sons, Inc., 2004. – 403 p.
8. Cook C. E. Radar signals: An introduction to theory and application / C. E. Cook, M. Bernfeld. – Boston: Artech House, 1993. – 552 p.
9. McDonough R. N. Detection of signals in noise (2nd. Ed.) / R. N. McDonough, A. D. Whalen. – San Diego : Academic Press, Inc., 1995. – 495 p.
10. Mathematical model of a two-fragment signal with a nonlinear frequency modulation in the current period of time / [O. O. Kostyria, A. A. Hryzo, O. M. Dodukh et al.] // Visnyk NTUU KPI Seriia – Radiotekhnika Radioaparatobuduvannia. – 2023. – Vol. 92. – P. 60–67. DOI: 10.20535/RADAP.2023.92.60-67.
11. Improvement of mathematical models with time-shift of two- and tri-fragment signals with non-linear frequency modulation / [O. O. Kostyria, A. A. Hryzo, O. M. Dodukh et al.] // Visnyk NTUU KPI Seriia – Radiotekhnika Radioaparatobuduvannia. – 2023. – Vol. 93. – P. 22–30. DOI: 10.20535/RADAP.2023.93.22-30.
12. Implementation of the method of minimizing the side lobe level of autocorrelation functions of signals with nonlinear frequency modulation / [O. O. Kostyria, A. A. Hryzo, I. A. Khizhnyak, et al.] // Visnyk NTUU KPI Seriia – Radiotekhnika Radioaparatobuduvannia. – 2024. – Vol. 95. – P. 16–22. DOI: 10.20535/RADAP. 2024.95.16-22
13. Mathematical model of shifted time of combined signal as part of fragments with linear and quadratic frequency modulation / [O. O. Kostyria, A. A. Hryzo, Yu. S. Solomonenko, et al.] // Visnyk NTUU KPI Seriia – Radiotekhnika Radioaparatobuduvannia. – 2024. – Vol. 97. – P. 5–11. DOI:10.20535/RADAP.2024.97.5-11
14. Adithya V. N. Modified radar signal model using NLFM / V. N. Adithya, R. D. Elizabath, C. Kavitha // International Journal of Recent Technology and Engineering (IJRTE). – 2019. – Vol. 8, Issue 2S3. – P. 513–516. DOI: 10.35940/ijrte.b1091.0782s319
15. Anoosha Ch. Peak sidelobe reduction analysis of NLFM and improved NLFM radar signal with non-uniform PRI / Ch. Anoosha, B. T. Krishna // Aiub Journal of Science and Engineering (AJSE). – 2022. – Vol. 21, Issue 2. – P. 125–131.
16. Non-continuous piecewise nonlinear frequency modulation pulse with variable sub-pulse duration in a MIMO SAR radar system / [Yu. Zhaoa, M. Ritchieb, X. Lua et al.] // Remote Sensing Letters. – 2020. – Vol. 11, Issue 3. – P. 283–292. DOI: 10.1080/2150704X.2019 .1711237
17. Optimized multi-parameter NLFM pulse compression waveform for low time-bandwidth radar / [A. C. van-Zyl, E. A. Wiehahn, J. E. Cillers et al.] // International Conference on Radar Systems, 2022. – P. 289–294. DOI: 10.1049/icp.2022.2332.
18. Fan Z. Coded excitation with nonlinear frequency modulation carrier in ultrasound imaging system / Z. Fan, H. Meng // 2020 IEEE Far East NDT New Technology & Application Forum. – Kunming, Yunnan province, China: conference paper: IEEE, 2020. – P. 31–35. DOI: 10.1109/FENDT50467.2020.9337517.
19. Adithya V. N. Performance analysis of NLFM signals with Doppler effect and background noise / V. N. Adithya, R. D. Elizabath, C. Kavitha // International Journal of Engineering and Advanced Technology (IJEAT). – 2020. – Vol. 9, Issue 3. – P. 737–742. DOI: 10.35940/ijeat. B3835.029320
20. Analytic NLFM waveform design with harmonic decomposition for synthetic aperture radar / [Y. Zhang, Y. Deng, Z. Zhang et al.] // IEEE Geoscience and Remote Sensing Letters, 2022. – Vol. 4, Article no 4513405. DOI: 10.1109/lgrs.2022.3204351
21. A two-step optimization framework for low sidelobe NLFM waveform using fourier series / [Q. Xie, H. Zeng, Z. Mo et al.] // IEEE Geoscience and Remote Sensing Letters, 2022. – Vol. 19, Article no 4020905. DOI: 10.1109/LGRS.2022.3141081
22. Pulse-agile waveform design for nonlinear FM pulses based on spectrum modulation / [R. Zhuang, H. Fan, Y. Sun et al.] // IET International Radar Conference, 2021. – P. 964–969. DOI: 10.1049/icp.2021.0700.
23. Research on ultra-wideband NLFM waveform synthesis and grating lobe suppression / [L. Shuyi, Y. Jia, Y. Liu et al.] // Sensors. – 2022. – No. 24, Article number 9829. DOI: 10.3390/s22249829
24. Swiercz E. Estimation and classification of NLFM signals based on the time-chirp / E. Swiercz, D. Janczak, K. Konopko // Sensors. – 2022. – Vol. 22, Issue 21, Article no 8104. DOI: 10.3390/s22218104
25. A variable chirp rate stepped frequency linear frequency modulation waveform designed to approximate wideband non-linear radar waveforms / [M. Saleh, S.-M. Omar, E. Grivel et al.] // Digital Signal Processing. – 2021. – Vol. 109, Article no 102884. – 19 p. DOI: 10.1016/j.dsp.2020.102884
26. Xu Z. Nonlinear frequency-modulated waveforms modeling and optimization for radar applications / Z. Xu, X. Wang, Y. Wang // Mathematics. – 2022. – Vol. 10. – P. 3939. DOI: 10.3390/math10213939.
27. Analysis of non linear frequency modulation (NLFM) waveforms for pulse compression radar / [M. R. Widyantara, S.-F. Y. Suratman, S. Widodo et al.] // Jurnal Elektronika dan Telekomunikasi. – Vol. 18, Issue 1. – P. 27–34. DOI: 10.14203/jet.v18.27-34
28. PHS: A pulse sequence method based on hyperbolic frequency modulation for speed measurement / [T. Ping, C. Song, Z. Qi et al.] // International Journal of Distributed Sensor Networks. – 2024. – Vol. 2024, Article no 6670576. – 11 p. DOI:10.1155/2024/6670576
29. Magneto-Acousto-Electrical Tomography using Nonlinearly Frequency-Modulated Ultrasound / [Z. Cheng, Z. Sun, J. Wang et al.] // Phys. Med. Biol. – 2024. – Vol. 69(8), PMID: 38422542. DOI:10.1088/1361-6560/ad2ee5

DOI 10.15588/1607-3274-2025-1-2

30. Singh A. K. NLFM pulse radar for drone detection using predistortion technique / A. K. Singh, K.-B. Bae, S.-O. Park // Journal of Electromagnetic Waves and Applications. – 2021. – Vol. 35. – P. 416–429.
31. Septanto H. A novel rule for designing tri-stages piecewise linear NLFM chirp / H. Septanto, O. Sudjana, D. Suprijanto // 2022 International Conference on Radar, Antenna, Microwave, Electronics, and Telecommunications (ICRAMET), Bandung, 6–7 December 2022. – Indonesia: IEEE, 2022. – P. 62–67. DOI: 10.1109/ICRAMET 56917.2022.9991201
32. Kostyria O. O. Combined two-fragment radar signals with linear and exponential frequency modulation laws / O. O. Kostyria, A. A. Hryzo, O. M. Dodukh // Systems of Arms and Military Equipment. – 2024. – № 4 (76). – P. 58–64. DOI: 10.30748/soivt.2023.76.06
33. Kostyria O. O. Synthesis time-shifted mathematical model of a combined signal with linear and cubic frequency modulation / O. O. Kostyria, A. A. Hryzo, O. M. Dodukh // Information Processing Systems. – 2024. – № 1 (176). – P. 73–81. DOI:10.30748/soi.2024.176.09
34. Synthesis of a single-channel device for receiving and primary signal processing under conditions of structural-parametric a priori uncertainty / [M. Kaliuzhnyi, V. Semenets, V. Orlenko et al.] // 2022 IEEE 2nd Ukrainian Microwave Week (UkrMW). – Ukraine: IEEE, 2022. – P. 573–578, DOI: 10.1109/UkrMW58013.2022. 10037164
35. Feller W. An introduction to probability theory and its applications, Volume 2 / W. Feller. – New York: John Wiley & Sons Inc., 1991. – 683 p.
36. Stacy E. W. A generalization of the gamma distribution / E. W Stacy // Annals of Mathematical Statistics. – 1962. – Vol. 33(3). – P. 1187–1192. DOI: 10.1214/aoms/ 1177704481
37. Alzaatreh A. Family of generalized gamma distributions: Properties and applications / A. Alzaatreh, C. Lee, & F. Famoye // Hacettepe Journal of Mathematics and Statistics. – 2016. – Vol. 45(3). – P. 869–886. DOI:10.15672/ HJMS.20156610980
38. Kiche J. On generalized gamma distribution and its application to survival data / J. Kiche, O. Ngesa, & G. Orwa // International Journal of Statistics and Probability. – 2019. – Vol. 8(5). – P. 85–102. DOI: 10.5539/ijsp.v8n5p85
39. Sportouche H. Mimic capacity of fisher and generalized gamma distributions for high-resolution SAR image statistical modeling / H. Sportouche, J.-M. Nicolas, F. Tupin // IEEE Journal of Selected Topics in Applied Earth Observations and Remote Sensing. – 2017. – Vol. 10, Issue 12. – P. 5695–5711
40. Thakur A. Transmit waveform design to avoid target masking in pulse compression radar / A. Thakur and D. S Saini // 2020 International Conference on Communication and Signal Processing (ICCSP), Chennai. – India, 2020. – P. 97–101. DOI:10.1109/ICCSP48568.2020. 9182221
41. Sidelobe suppression with resolution maintenance for SAR images via sparse representation / [X. Zhu, F. He, F. Ye et al.] // Sensors (Basel). – 2018. – Vol. 18(5), Article no1589. DOI: 10.3390/s18051589; PMID: 29772743; PMCID: PMC5982680.
42. Haliloglu O. Successive target cancelation in pulse compression radars / O. Haliloglu, A. O. Yilmaz // 2007 IEEE Radar Conference, Waltham. – MA, USA: IEEE, 2007. – P. 885–890. DOI: 10.1109/RADAR.2007.374336
43. A simulation of study of the impact of surface clutter on spaceborne precipitation radar sensor / [R. Nepal, Z. Li, Y. Zhang et al.] // In Proceedings of the 36th Conference on Radar Meteorology, Breckenridge. – CO, USA: IEEE, 2013. – P. 16–20.
44. Maki M. Construction of three-dimensional weather radar data from volcanic eruption clouds / M. Maki, T. Kobori // MethodsX. – 2021. – Vol. 8, Article no 101535. DOI: 10.1016/j.jvolgeores.2021.107178

DOI 10.15588/1607-3274-2025-1-2